Chapter 2

Seismic Crack Investigation in an Earth Dam by Centrifugal Loading Test

Akira Kobayashi and Akira Murakami

Additional information is available at the end of the chapter

http://dx.doi.org/10.5772/intechopen.78788

Abstract

There are many Earth-fill dams in Japan, which are mostly used for irrigation use. Most of these dams in Japan were constructed by experience over 100 years ago. There are so many irrigation dams, which suffered earthquake damage in the past. Due to the damages, the cracks at the crest in the dam-axis direction have been reported in many cases. For the rock-fill dam recently constructed, the crack on the crest in the dam-axis direction has also been found in the case of a large earthquake. The mechanism of such a crack has not been discussed well. In this study, to clarify the mechanism of a crack in the dam-axis direction, a centrifugal loading test was applied to the dam with a 50 G gravity field. As a result, the critical level of strain was observed at the crest of the model, and it was found that the horizontal displacement at the upper part of the dam was excessive. It can be concluded from the study that the seismic cracks in the dam-axis direction occurred due to the excessive tensile stress, which was not considered in the design process.

Keywords: Earth and rock-fill dam, earthquake damage, crack, centrifugal loading test, image analysis

1. Introduction

In Japan, there are approximately two hundred 10,000 small-Earth dams, which have significant reservoirs for irrigation. Such kinds of dams whose heights are smaller than 15 m are called irrigation dams. Many irrigation dams were constructed by experience over 100 years ago. It is reported that about 20,000 irrigation dams were damaged during the long-term use, which need repairing and strengthening [1].

Many irrigation dams were not designed for earthquake resistance, and the cracks at the crest in the direction of the dam axis are remarkable. **Figure 1** shows the example of the crack at the crest of the Earth-fill dam. The relatively big open crack occurred. This type of open crack can be seen in the damaged Earth-fill dam so often. Not only the old Earth-fill dam but also the recent rock-fill dam has a crack in the dam-axis direction when the big earthquake hit. **Figure 2** shows the crack situation at the crest of the rock-fill dam constructed in 1988. This dam was designed for earthquake resistance. Although the acceleration was not measured, it was inferred that relatively big acceleration occurred because the earthquake inducing the crack was in 2011 off the Pacific coast of Tohoku. The open crack was propagated at a 3 m depth from the crest. The cracks shown in the figures cannot be seen to be induced by shear failure. The earthquake resistance is examined for shear failure with the slip-circle method according to the standard. It is difficult to

Figure 1. Crack at the Earth-fill dam.

Figure 2. Crack at the rock-fill dam.

http://dx.doi.org/10.5772/intechopen.78788

repair the damaged dam effectively when the mechanism of the crack on the crest is not clarified. On the contrary, if the mechanism becomes clear, an effective counterplan may be considered.

In this chapter, the centrifuge loading test is carried out to confirm the mechanism of the crack at the crest. Although the authors already carried out the 1-G shaking test and inferred that the tensile stress is the reason for the crack by observing the behavior of the cross section [3], this study aims to confirm more concretely the reason. Therefore, the centrifuge loading test of 50 G was planned to simulate the more realistic situation and the observation from the vertical direction also tried to observe the crack situation. Moreover, the simple numerical simulation has tried to reproduce the experimental results.

2. Previous studies

The 1-G shaking table tests were carried out to investigate the dam and embankment behavior, and it was found that the acceleration response at the upper part of the embankment has a large effect on the behavior of the slope [3]. The crack in the dam-axis direction was also examined and the crack was considered to be caused by tensile stress. The tensile stress was affected by the vertical vibration as well as horizontal one [4]. Like others, the relation between the natural period and failure feature was investigated [5]. The effect of the aspect ratio of the dam on the vibration mode was also examined [6].

For the centrifugal loading tests, the acceleration response and residual deformation were investigated for the Earth-core rock-fill dam and concrete-faced rock-fill dam [7]. The effect of the liquefaction of foundation on the deformation of the dam was examined [8]. Moreover, the seismic response and liquefaction of loose embankments were also investigated [9].

As mentioned earlier, the previous studies focused on the seismic response, slope sliding and deformation and so the situation of the surface of the dam was focused. On the other hand, the authors investigated the behavior of the cross section by 1-G shaking table test [2] as mentioned earlier. **Figure 3** is the strain distribution of the model used for 1-G shaking table test. By using

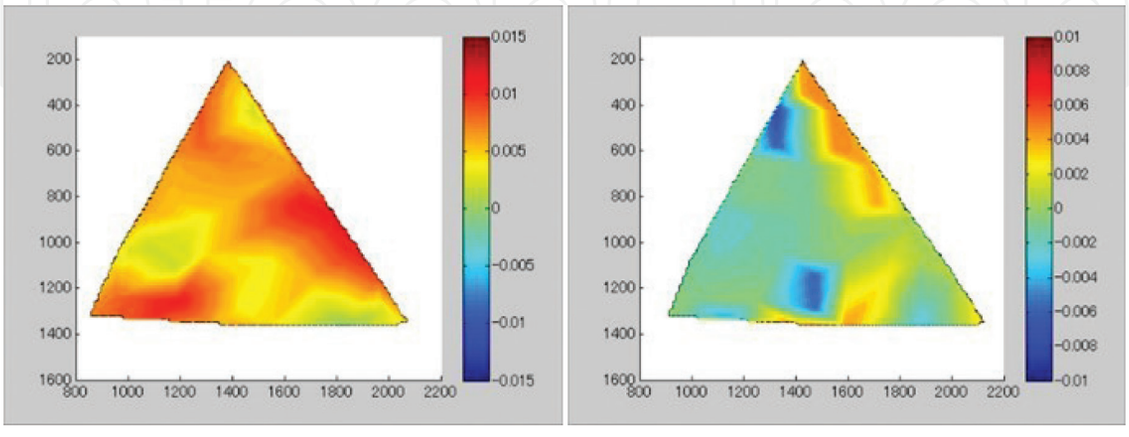

Figure 3. Strain distribution by 1-G shaking test [2]: (a) shear strain and (b) volumetric strain.

image analysis, the behavior of cross section was observed. It was found that the share stain became large at the slope, and the large volumetric strain was observed at the upper part of the dam. In this study, a similar image analysis is used for the centrifugal loading test.

3. Centrifugal loading test

3.1. Test conditions

The centrifugal loading tests were conducted under 50-G with a 1/50 scaled model. In this experiment, the model with a height of 100 mm and upstream and downstream gradients of 1:1 was used. **Figure 4** shows the schematic view of the model. The model was made from

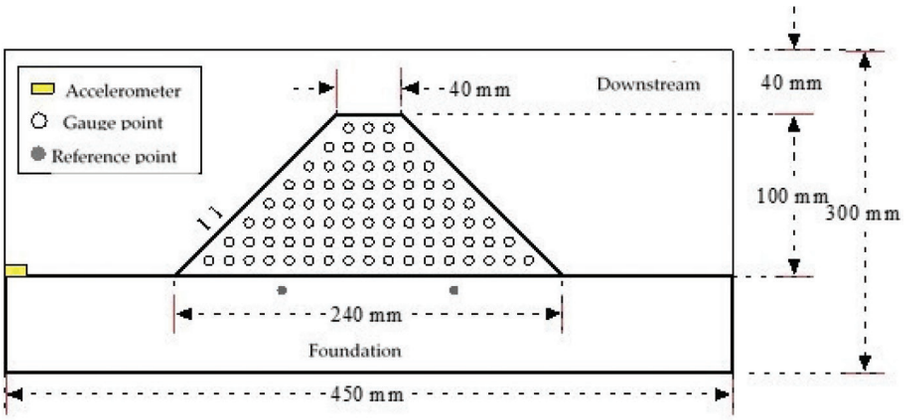

(a)

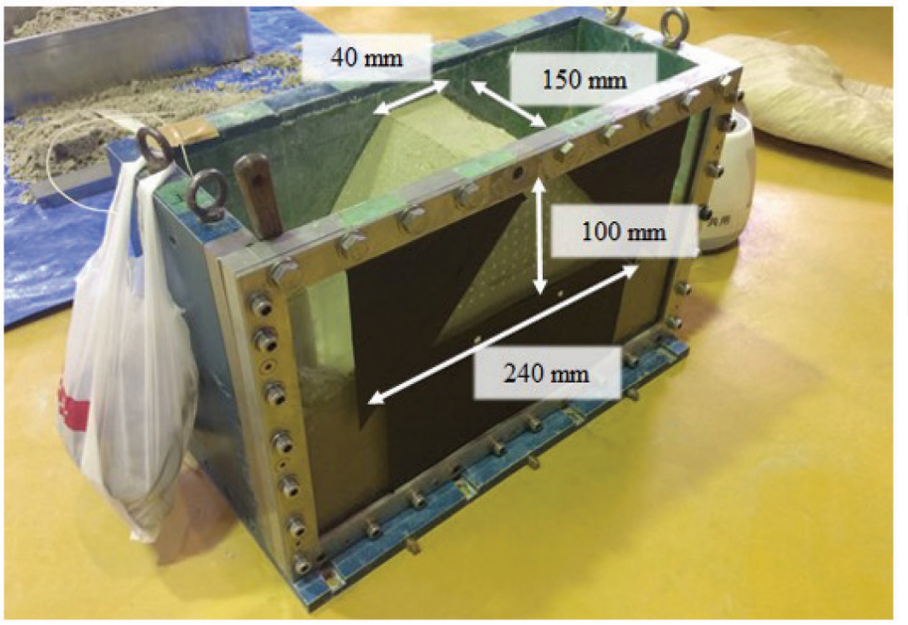

(b)

Figure 4. Schematic view of the model and soil box for centrifugal loading test. (a) Schematic view of the model; and (b) the situation of soil box for centrifugal loading test.

No. 7 silica sand and kaolin clay with the mixture ratio of 8:2 by dry weight. **Figure 5** shows the particle distribution of the mixture. The water content of the mixture was 13%. In order to evaluate the seismic behavior of the model, the gauge points were placed on the surface of the embankment model and the reference points were set at the foundation. The total number of the points is 82. To reduce the friction between embankment model and wall of the soil box, the silicone grease was painted on the wall surface. The accelerometers were installed on the foundation. The foundation was made of rigid material. By assuming that the distance of the reference points on the rigid foundation is not changed, the coordinate of the gauge points is calibrated.

The model was excited with a horizontal sine wave of 50 Hz whose amplitude is 1.5 mm. The input seismic wave corresponds to the earthquake ground motion with a peak acceleration of about 300 gal, and the frequency is 1 Hz.

3.2. Digital image analysis

In order to evaluate the displacement of the gauge points, the digital image analysis method used in the 1-G shaking table test [2] is applied.

Firstly, the static image is taken before the model is tested. While the model is excited, continuous images are taken by the high-speed camera of which the shooting speed is 1000 fps. The images are transformed into black and white binary images. The noise reduction is, then, carried out as shown in **Figure 6**. The number of the points is confirmed to be 82 at this stage. Then, the coordinates of the gauge points are measured in the unit of pixels by calculating the center position of each white element representing the gauge point. Finally, the distance between two reference points at the foundation, which was precisely 150 mm, is measured in the unit of pixels. The scale calibration is carried out by the distance of reference points and the coordinate of the gauge points is calculated as the relative location of the reference point in the unit of mm. By repeating this procedure for all dynamic images, the displacement variation of each gauge point can be obtained.

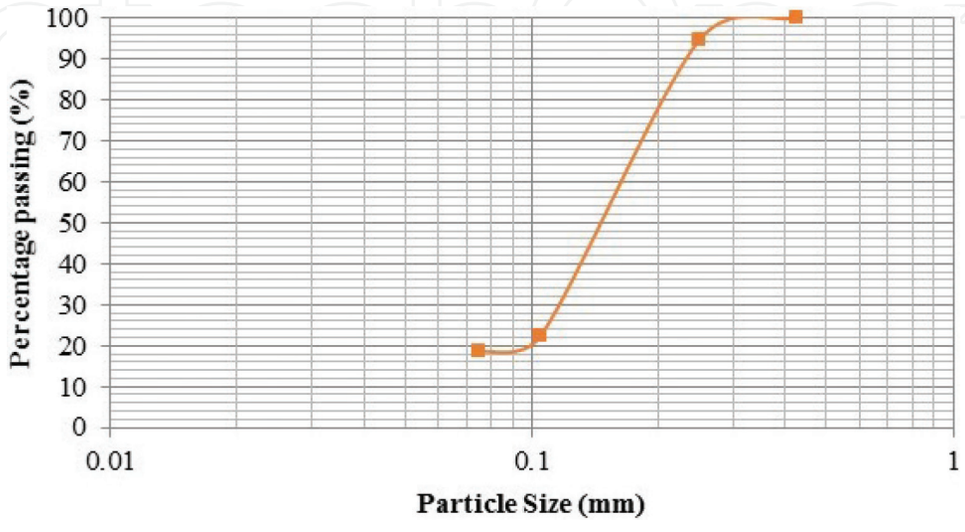

Figure 5. Particle size distribution used for the embankment model.

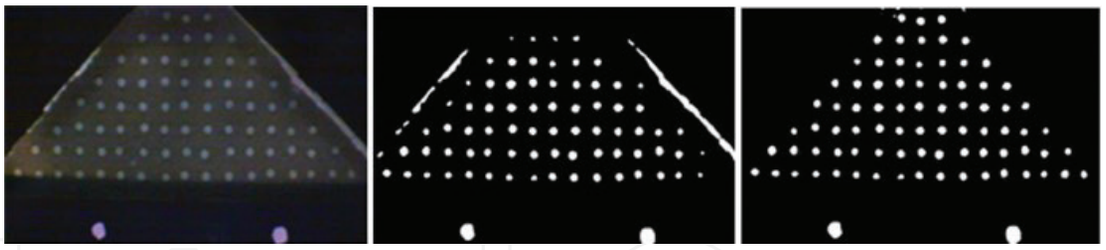

Figure 6. Examples of image analysis process: (a) picture image; (b) binary image; and (c) noise reduction result.

3.3. Calculation of strain

As the gauge points are regarded as the nodes, the cross section is discretized with a triangular element. By using the plane strain condition, the shear and volume strains are calculated for each element with the theory of the finite element method.

4. Experimental results

4.1. The behavior of cross section

By using the method mentioned above, the behavior of the cross section is examined. **Figure 7** shows the final displacement vector distribution after experiment and the situation of cracks. The cracks occurred at the upper part of the dam body of which the situation is explained later. The downward displacement vector is large at the upper part while the displacement at the lower part is minimal.

The gauge points shown by the number in **Figure 8** are focused on highlighting the deformation pattern. The downward displacement at the vertical centerline of the dam body, of which

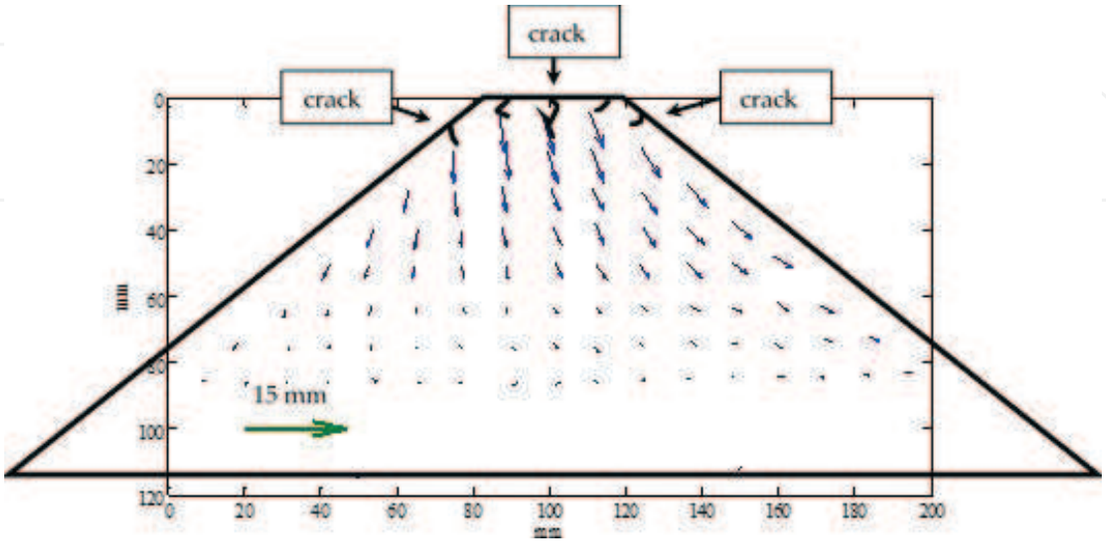

Figure 7. Displacement vector distribution after experiment.

http://dx.doi.org/10.5772/intechopen.78788

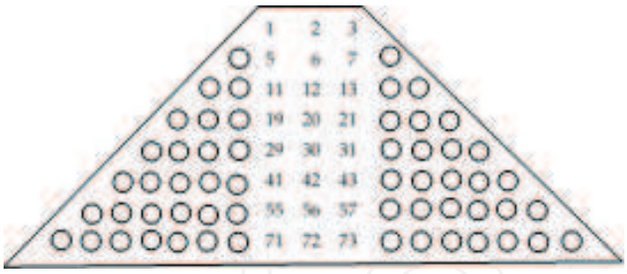

Figure 8. Number of gauge points highlighted for observation.

the number is from 2 to 72, is shown in **Figure 9**. To observe the tendency of the settlement, the displacement is averaged with the period of 0.02 s which is the same as the period of shaking. The downward displacement becomes gradually large with the height of the gauge point. The deformation continues during the experiment at the upper part while the displacement at the lower part does not change so much during the experiment. It is found that the deformation of the upper part occupies the settlement of the dam.

Then, to observe the horizontal deformation, the change in the horizontal distance between two gauge points is investigated. For example, at the upper most part of the dam, the horizontal distance of gauge points 1 and 3 is presented (see **Figure 8**). **Figure 10** shows the change in the horizontal distances at various heights of the dam with time, in which the legend means the number of gauge points used for the distance calculation. While the horizontal distance becomes large at the height of the middle, the number of 29–31, at the early stage, the ones at the upper parts, the number of 1–3 and 5–7, gradually increase with time. The upper parts have a significant change in the horizontal distance finally. Entirely, the center part of the dam has the horizontal tension behavior except for the lowest part.

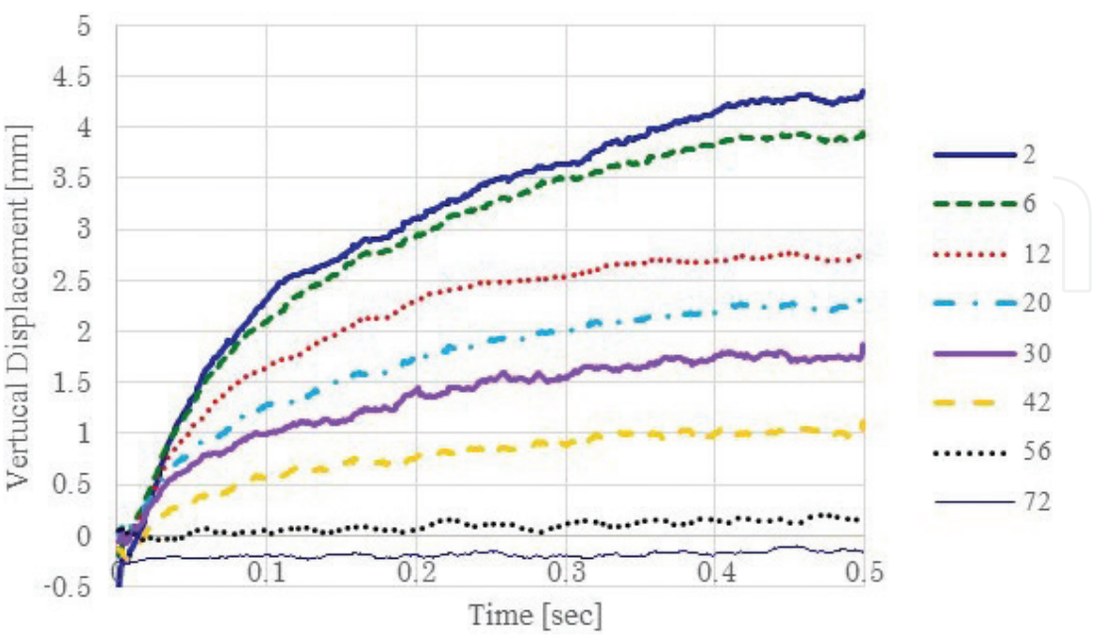

Figure 9. Downward displacement at the centerline of the dam.

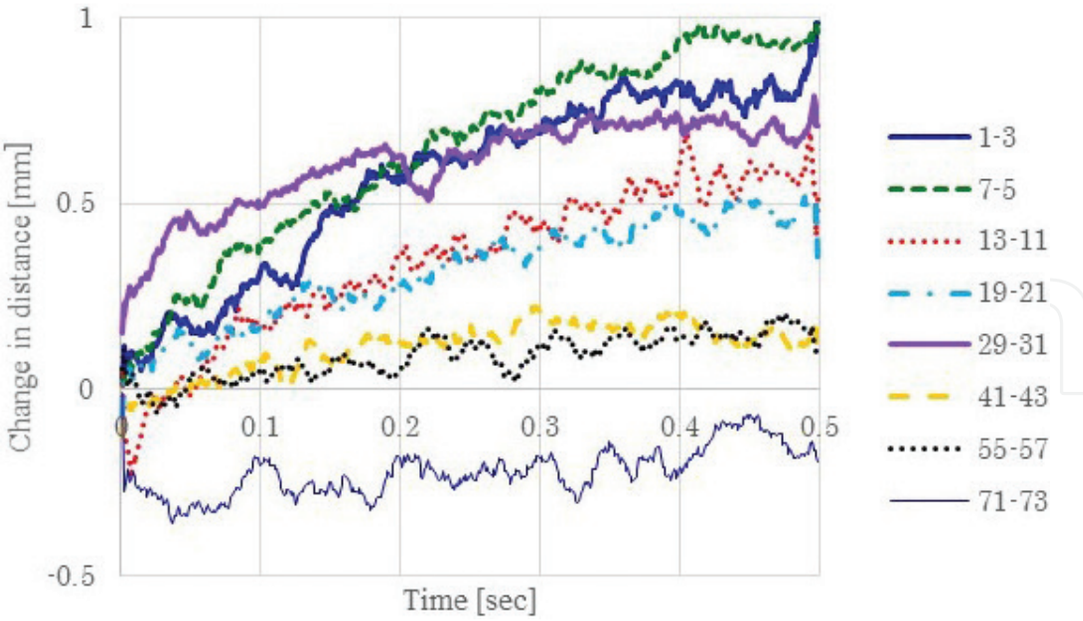

Figure 10. Change in the horizontal distance at the centerline of the dam.

Figure 11 shows the change in shear strain distribution. The situation starts from the left end of shaking, moves to the center and right end, and then reverses to the center and finally returns to the left end. The positive value means the shear strain at downstream shown in **Figure 4(a)**, which coincides with the right-hand side. The time

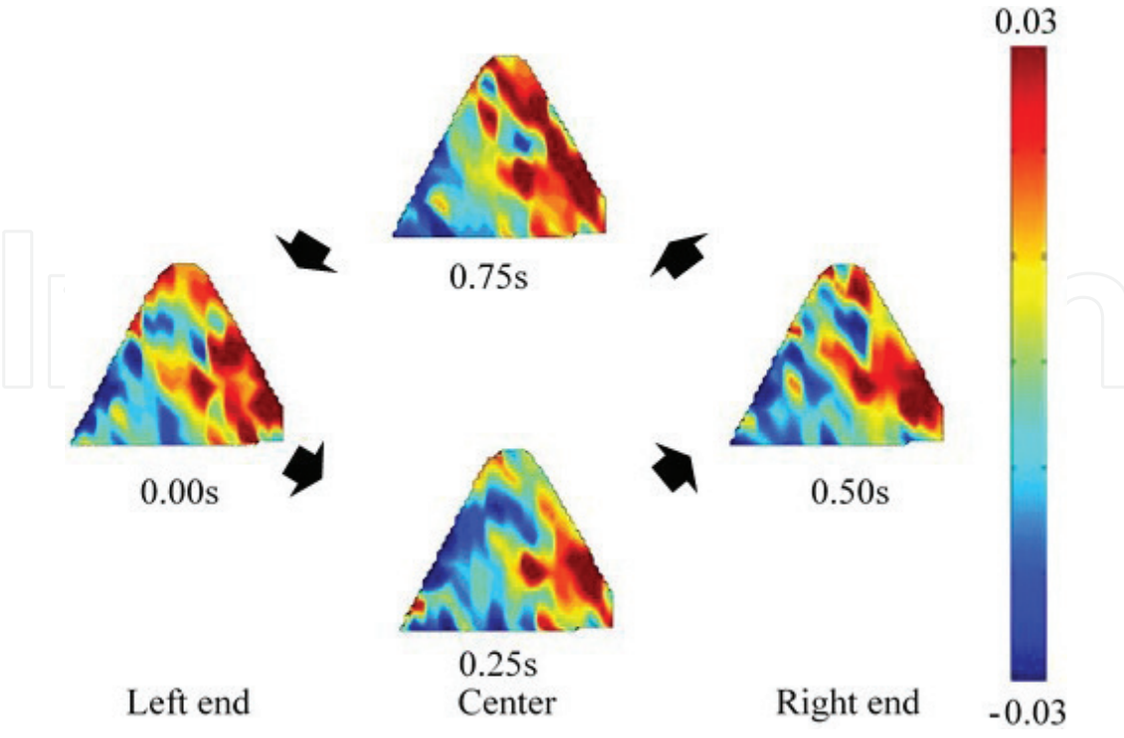

Figure 11. Change in shear strain distribution.

http://dx.doi.org/10.5772/intechopen.78788

means the corresponding actual one. The shear strain to upstream direction occupies the upstream lower part, while the downstream side of the dam shows the shear strain at the downstream direction. The shear strain in both directions becomes larger at the lower part than the upper part.

Figure 12 indicates the volumetric strain distribution change. The positive value means the extension. It is found that the extension occurs at the upper part during the shaking. At the lower part, the extension and compression distribute apparently, and so the striped pattern can be seen. It is shown that the part showing the extension strain coincides with the part indicating the horizontal tension behavior explained (see **Figure 11**).

4.2. Behavior of crest

The situation of the crest after the test is shown in **Figure 13**. The crack is marked with the red line. The crack in the dam-axis direction can be seen at the center of the crest as shown at the actual damage site. The sliding behavior cannot be found at the slope of the dam. In order to investigate the deformation situation at the crest, an additional experiment is carried out, at which the gauge points are set at the crest and slope as shown in **Figure 14**. As the situation was photographed from the top, the strain is estimated just for the horizontal plane (**Figure 15**). Therefore, the obtained strain is not the one on the slope but the apparent strain on the horizontal plane. Only the strain distribution at the crest is the accurate value as a strain.

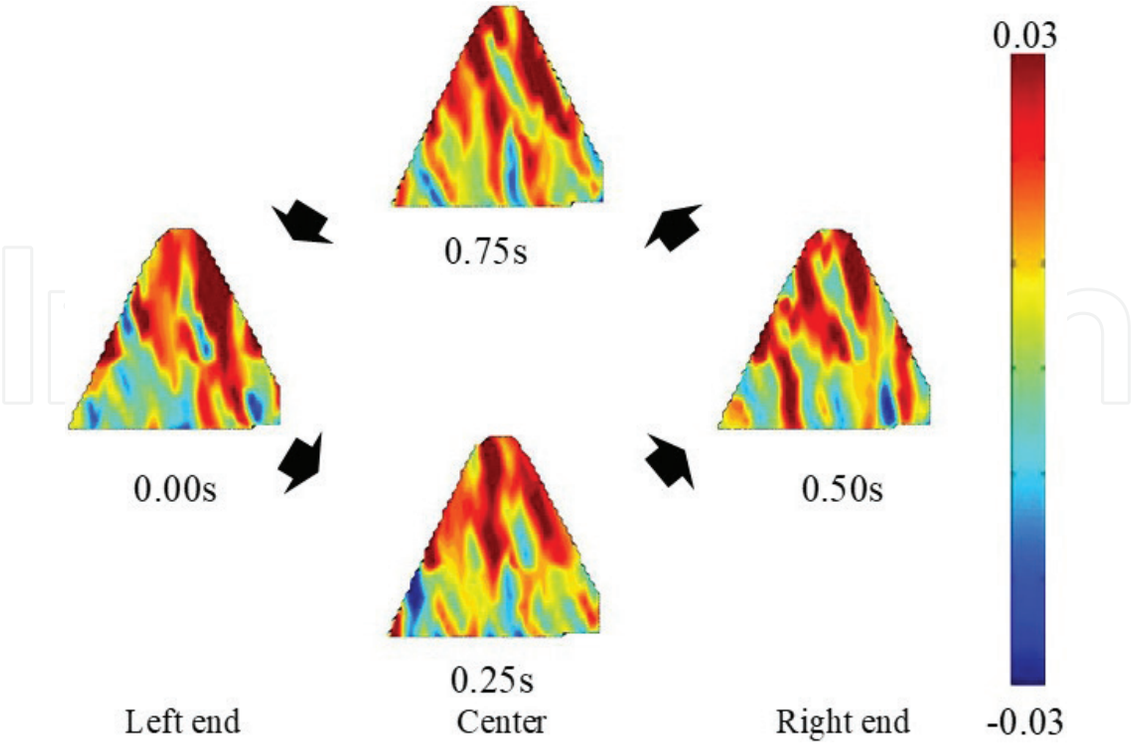

Figure 12. Change in volumetric strain distribution.

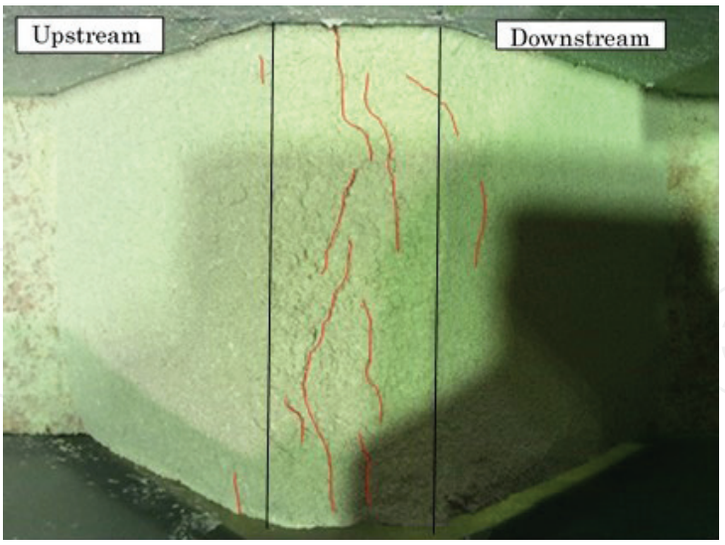

Figure 13. Cracks at the crest after the experiment.

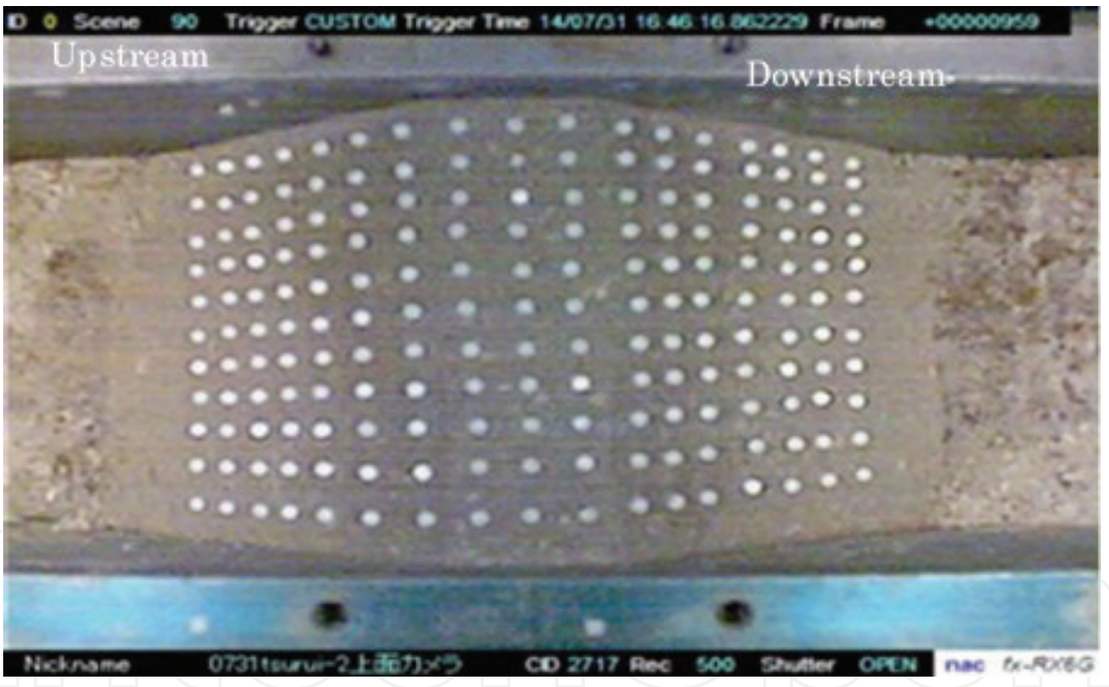

Figure 14. The gauge points on the crest and the slope. (a-1) Left end: shear strain; (a-2) left end: volumetric strain; (b-1) center: shear strain; (b-2) center: volumetric strain; (c-1) right end; shear strain; (c-2) right end: volumetric strain; (d-1) center: shear strain; (d-2) center: volumetric strain.

The shear strain is shown to develop to the upstream and downstream direction near the wall of the sand box. These results may be caused by the friction between wall and dam model. The direction of shear strain distributes alternatively, and the large shear strain develops in the upstream and downstream direction.

http://dx.doi.org/10.5772/intechopen.78788

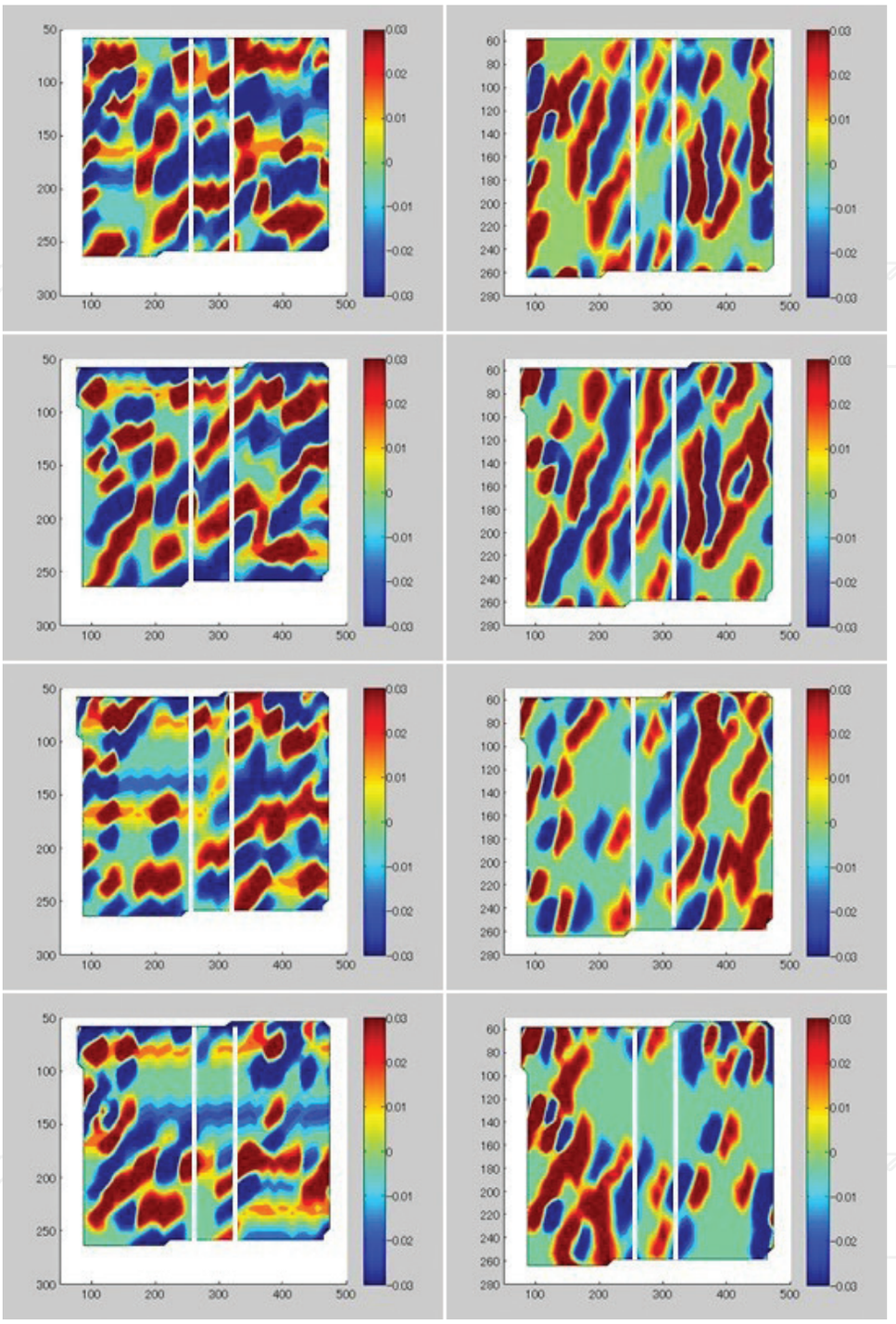

Figure 15. Shear and volumetric strain at the crest and slope.

On the other hand, while the volumetric strain also shows the stripe pattern, the direction of the strain development is dam-axis one, which coincides with the crack situation shown in **Figure 13**. It can be found that the crack shown in **Figure 13** is caused by the extension strain at the crest.

4.3. Summary of the experiment

It can be concluded from the experimental results as follows:

1. The cracks in the dam-axis direction can be realized by the experiment. Such a crack shown at the earthquake damage is caused by the extension strain. Therefore, the extension stress is caused by the parts of the crest. While the extension failure is not examined in the design process, the counterplan may be necessary as the earthquake resistance.
2. The shear strain at the cross section developed to the slope direction. While the shear strain distribution coincided with the sliding failure of the slope, the failure form by sliding was not observed.

5. Numerical examination

5.1. Conditions

To investigate the reproducibility of the extension strain distribution by numerical simulation, the dam model of which size is the same as the 1-G shaking test [2] is simulated. In this study, two cases are examined. The first one is the case in which the dam body is directly shaken at the bottom of the dam. The second one is the case in which the thin base is added under the dam. The objective of the second case is to input the inhomogeneous wave into the dam body. When a given wave is subjected to the bottom of the base, the shaking of the bottom of the dam body becomes a little inhomogeneous, while the amplitude is not so different. The dam body has a height of 150 mm and upstream and downstream gradients of 1:0.545. As the slope gradient is steep, the shaking would be intensified at the upper part.

To examine the strain distributions, the elasto-plastic finite element method (FEM) using Mohr-Coulomb's criteria as the yield function is applied in this study. The bottoms of the models are subjected to 2.4 Hz of a horizontal sine wave. The amplitude is 280 gal.

Figure 16 shows the schematic view of the models and **Table 1** indicates the material properties. By setting the elastic modulus of the base a little smaller than that of the dam, the shaking situation at the bottom of dam body becomes inhomogeneous by the different behavior of reflected wave depending on the location.

5.2. Results

Figure 17 shows the shear strain distribution and **Figure 18** indicates the volumetric strain distribution at the time when the model locates the center of shaking from downstream to upstream. It is found that the large shear strain occurs at the lower part for both cases while the direction is different for the case. Although Case 1 shows that the shear strain to the same direction occurs, the shear strain to the different direction is distributed for Case 2. For the volumetric strain, the maximum value is shown at the top and both ends of the bottom, and

http://dx.doi.org/10.5772/intechopen.78788

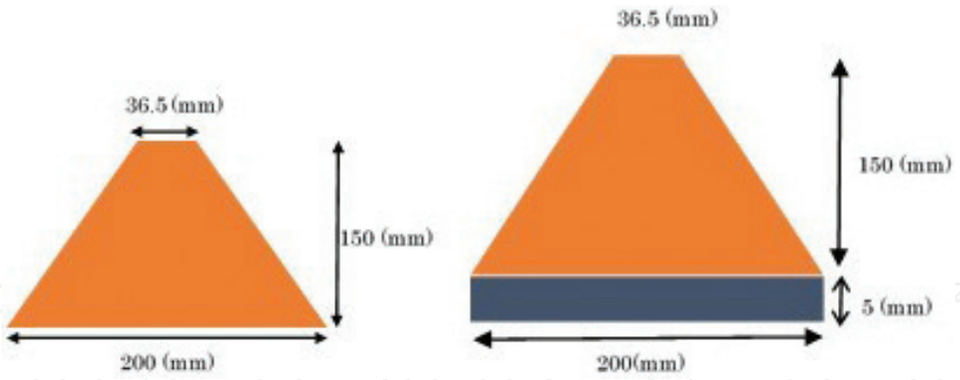

Figure 16. Model size of the numerical simulation. (a) Case 1 and (b) Case 2.

Parameters	Dam body	Base (Case 2)
Cohesion (kPa)	15	15
Unit weight (kN/m^3)	18	18
Elastic modulus (kPa)	3000	2850
Internal friction angle (°)	35	35
Poisson's ratio	0.3	0.3

Table 1. Material parameters used for numerical analysis.

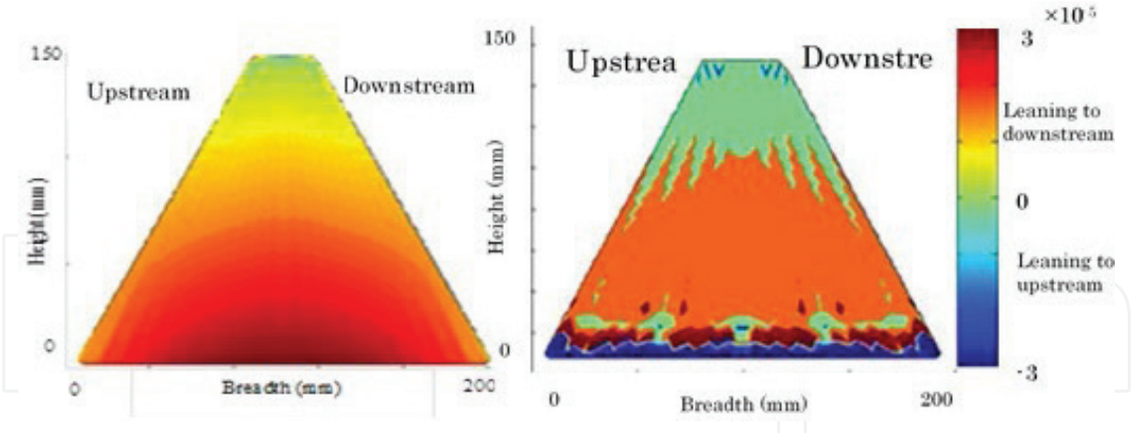

Figure 17. Shear strain distribution of the numerical simulation. (a) Case 1 and (b) Case 2.

the upstream side has the compression strain, and the downstream side has the extension strain for Case 1. On the other hand, Case 2 shows that the extension and compression strain distribute alternatively. This stripe pattern can be seen in the centrifugal loading test as shown in **Figure 12**. However, the large extension strain cannot be seen in the numerical simulation.

As a result of the numerical simulation, the analysis results are different from the experimental results. In particular, the large extension strain at the upper part cannot be realized by the

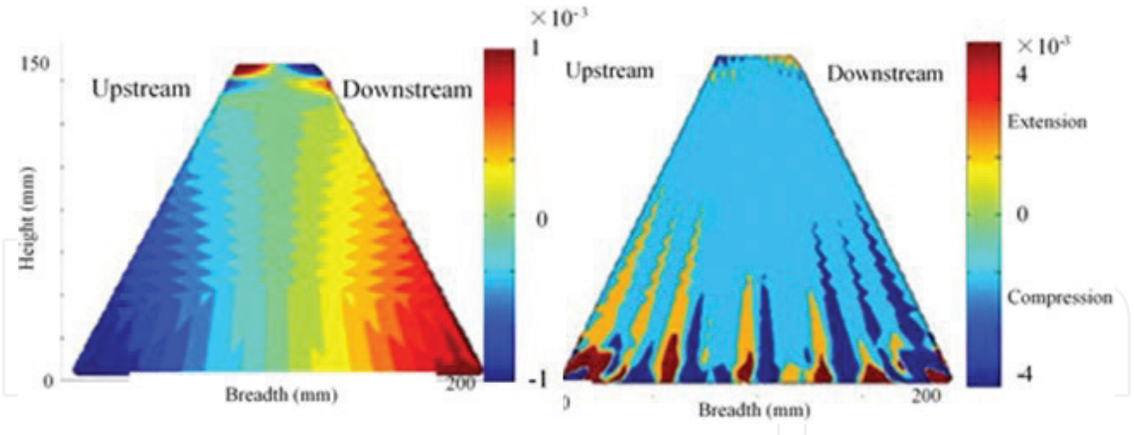

Figure 18. Volumetric strain distribution of the numerical simulation. (a) Case 1 and (b) Case 2.

analyses. The distribution of the shear strain is also quite different from the observed one. As a present conclusion, the ordinary elasto-plastic model is not suitable for the dynamic analysis of the dam.

6. Discussions

Many Earth dams had the cracks in the direction of dam axis at the crest when a big earthquake happened. In this study, to examine the mechanism of the cracks along the dam axis, the centrifugal loading tests are conducted. Moreover, numerical analyses are used to examine the mechanism theoretically.

It was found from experimental examination that the cracks in dam-axis direction shown as the earthquake damage were caused by the extension strain. Therefore, the extension stress was caused by the parts of the crest. However, the large extension strain at the upper part could not be realized by numerical analyses. This means that the cracks in the dam-axis direction cannot be explained theoretically at present.

While the extension failure is not examined in the design process, the counterplan for the cracks is necessary as the earthquake resistance. It is, however, difficult to examine the efficiency because it is impossible that the extension stress at the upper part of the dam body cannot be evaluated properly at present.

The shear strain at the cross section is developed to the slope direction in the experiment. While the shear strain distribution coincided with the sliding failure of the slope, the failure form by sliding was not observed. On the other hand, the distribution of the shear strain by numerical analysis was quite different from the observed one. Although the earthquake-resistance is examined for shear failure by Newmark's method [10] or the method by Watanabe and Baba [11] in Japan, the discussion about the critical situation of the seismic behavior of the fill dam would be needed.

Acknowledgements

This study was carried out with the support of the grant in aid for scientific research (A) and (B) of JSPS. The experiments were assisted by Mr. Tsurui and Mr. Sugano who were the graduate students of Kyoto University at that time. We appreciate the financial and technical support.

Author details

Akira Kobayashi[1]* and Akira Murakami[2]

*Address all correspondence to: koba5963@kansai-u.ac.jp

1 Department of Civil, Environmental and Applied systems Engineering, Kansai University, Osaka, Japan

2 Kyoto University, Kyoto, Japan

References

[1] Kato T. Flood mitigation function and its stochastic evaluation of irrigation ponds. Bulletin of the National Research Institute of Agricultural Engineering. 2005;(44):1-22 (in Japanese)

[2] Miyanaga Y, Kobayashi A, Murakami A. 1-G model test with digital image analysis for seismic behavior of earth dam. Geotechnical Engineering Journal of the SEAGS & AGSSEA. 2015;**44**(2):27-34

[3] Lin ML, Wang KL. Seismic slope behavior in a large-scale shaking table model test. Engineering Geology. 2006;**86**:118-133

[4] Masukawa S, Yasunaka M, Kohgo Y. Dynamic failure and deformations of dam-models on shaking table tests. In: Proceedings of 13th World Conference on Earthquake Engineering; 2004; Vancouver Canada. Paper No. 2359

[5] Tsutumi H, Watanabe H, Ogata N, Shiomi S. Dynamic test for seismic design of fill-type dam. Tsuchi to Kiso. JGS. 1975;**23**(5):11-20 (in Japanese)

[6] Masukawa S, Yasunaka M, Hayashida Y. Shaking table tests by silicone rubber dam model with different ratio of crest length to dam height. Tsuchi to Kiso. JGS. 2008;**56**(10):16-19 (in Japanese)

[7] Kim MK, Lee SH, Choo YW, Kim DS. Seismic behaviors of earth-core and concrete-faced rock-fill dams by dynamic centrifuge test. Soil Dynamics and Earthquake Engineering. 2011;**31**:1579-1593

[8] Sharp MK, Adalier K. Seismic response of earth dam with varying depth of liquefiable foundation layer. Soil Dynamics and Earthquake Engineering. 2006;**26**:1028-1037

[9] Ng CWW, Li XS, Van Laak PA, Hou DYJ. Centrifuge modeling of loose fill embankment subjected to uni-axial and bi-axial earthquakes. Soil Dynamics and Earthquake Engineering. 2004;**24**:305-318

[10] Newmark NM. Effect of earthquakes on dams and embankments. Geotechnique. 1965; **15**(2):139-159

[11] Watanabe H, Baba K, Hirata K. A consideration on the method of evaluation for sliding stability of fill dams during strong motion earthquakes based upon dynamic analysis. CRIEPI Research Report. No. 381020. 1981 (in Japanese)